Correlation-enhanced electron-phonon interaction in a strongly correlated electron system

J. D. Lee, Kicheon Kang, and B. I. Min
Department of Physics, Pohang University of Science and Technology, Pohang 790-784, Korea
(Received 11 March 1994; revised manuscript received 18 July 1994)

In order to investigate effects of the Coulomb correlation on the electron-phonon interaction in a strongly correlated system, the electron-phonon coupling constant (λ_{ph}) and the electron-spin-fluctuation coupling constant (λ_{sf}) are evaluated for the Hubbard Hamiltonian system. It is found that the Coulomb correlation in the Hubbard model gives rise to a phonon hardening and an enhancement of λ_{ph}. Further, both λ_{ph} and λ_{sf} are found to be reduced significantly in overall magnitudes, if an effect of the finite bandwidth is taken into account. In particular, we have found that λ_{ph} becomes larger than λ_{sf} for a system with a nearly filled band, which indicates that a phonon-mediated BCS superconductivity may be possible in strongly correlated systems.

I. INTRODUCTION

It is a fundamental question whether the origin of superconductivity in high-T_c superconductors or heavy fermion systems is BCS-like or not. These systems are believed to be strongly correlated electron systems which have strong spin-fluctuation effects, and so the phonon-mediated BCS superconductivity is expected to be suppressed. Therefore a number of novel or exotic nonphonon superconducting mechanisms have been proposed.[1] However, there are several experiments which give direct evidence for a strong coupling between phonons and superconducting electrons in these systems.[2]

The BCS superconducting transition temperature for a spin-fluctuating system is a function of the effective coupling constant λ, which is given by

$$\lambda \simeq \frac{\lambda_{ph} - \lambda_{sf}}{1 + \lambda_{ph} + \lambda_{sf}}, \tag{1}$$

where λ_{ph} and λ_{sf} are electron-phonon and electron-spin-fluctuation coupling constant, respectively.[3] If $\lambda_{ph} \leq \lambda_{sf}$, the phonon-mediated BCS superconductivity is suppressed. It is well understood that λ_{sf} becomes significantly enhanced in a strongly correlated system [in the region of $IN(E_F) \rightarrow 1$: I and $N(E_F)$ correspond to the Coulomb correlation and the density of states at the Fermi level, respectively]. On the contrary, the behavior of λ_{ph} in correlated systems has not been exploited much.

For an electron gas system, Kim[4] has investigated effects of an exchange interaction on λ_{ph}, and found that a phonon softening and an enhancement of λ_{ph} occur due to the exchange interaction. Based on these findings, he suggested that superconductivity in heavy fermions or high-T_c superconductors may be caused by an exchange-enhanced electron-phonon interaction.[5]

Kim *et al.*[6] have studied the effect of very strong correlation on electron-phonon interactions and the implications for transport properties in the high-T_c superconductors. By viewing the copper oxide high-T_c superconductors as moderately heavy Fermi liquids, they argued that Coulomb correlations tend to suppress charge fluctuations within the copper oxides planes, and that the electron-phonon interaction becomes progressively weakened as the metal-insulator transition is approached. They concluded that the strength of the electron-phonon interaction appears to be too weak to be the primary mechanism responsible for high-T_c superconductivity. More recently, Kim and Tesanovic[7] have explored a phonon mechanism for high-T_c superconductors. Employing the slave boson formulation, they examined the concentration dependence of the Eliashberg electron-pair interaction function derived from the Hubbard model[8] in the $I \rightarrow \infty$ limit. They found that, at some critical concentration x_c, attractive interactions due to phonons completely cancel the repulsive interactions due to slave bosons, and the effective pair interaction becomes attractive for $x > x_c$, reflecting the possible phonon mechanism for superconductivity. In these formulations, there is no explicit dependence of the Coulomb correlation parameter I, because they considered the $I = \infty$ Hubbard model.

Motivated by the above suggestions, we have attempted to examine the electron-phonon interaction for the Hubbard model which is typical of strongly correlated electron systems such as high-T_c superconductors or heavy fermions. Employing the diagrammatic method, we have evaluated λ_{ph} and λ_{sf} on an equal footing, and discussed in detail behaviors of them with respect to the parameter $IN(E_F)$. We have found that a ladder-type diagram in the electron-phonon vertex function leads to the electron-phonon interaction matrix element strongly enhanced as $IN(E_F) \rightarrow 1$. We have also found that the spin-fluctuation effect is suppressed very much when the effect of a finite bandwidth is considered, yielding that λ_{ph} becomes dominant over λ_{sf}.

0163-1829/95/51(6)/3850(6)/$06.00

II. ELECTRON-PHONON COUPLING CONSTANT λ_{ph}

The model Hamiltonian in consideration is

$$H = \sum_{k\sigma} \epsilon_k c^\dagger_{k\sigma} c_{k\sigma} + \sum_q \Omega_q b^\dagger_q b_q + H_{\text{el-el}} + H_{\text{el-ph}}. \quad (2)$$

The first two terms are noninteracting electron and phonon Hamiltonians, respectively. $H_{\text{el-el}}$ and $H_{\text{el-ph}}$ represent the Hubbard-type electron-electron Coulomb correlation interaction and the electron-phonon interaction Hamiltonian, respectively, given by

$$H_{\text{el-el}} = \frac{I}{2} \sum_{kk'q} \sum_\sigma c^\dagger_{k+q\sigma} c_{k\sigma} c^\dagger_{k'-q,-\sigma} c_{k',-\sigma}, \quad (3)$$

$$H_{\text{el-ph}} = \sum_{kq} \sum_\sigma g(q) c^\dagger_{k\sigma} c_{k-q\sigma} (b_q + b^\dagger_{-q}), \quad (4)$$

where $g(q)$ in Eq. (4) is an electron-phonon interaction matrix element.

Let us first evaluate the phonon Green's function to determine the renormalized phonon frequency. We consider diagrams shown in Fig. 1 which represent Dyson's equation for the phonon Green's function. The single wavy line in Fig. 1(a) represents a noninteracting phonon Green's function, $D^0_q(i\nu_m) = 2\Omega_q/(\nu_m^2 + \Omega_q^2)$, while the double wavy line represents an interacting phonon Green's function, $D_q(i\nu_m)$, i.e., the Green's function in the presence of both electron-phonon and electron-electron interactions. Besides a usual bubble diagram [Fig. 1(b)] of a renormalized Coulomb correlation, we have also considered for the phonon self-energy the ladder diagram of Fig. 1(c) to account for a transverse spin-fluctuation effect. In fact, we have found that the contribution from Fig. 1(c) becomes dominant when $IN(E_F) \to 1$, as will be shown below.

A double-dotted line in Fig. 1(b) represents the renormalized Coulomb correlation

$$\tilde{I} = \frac{I}{1 + IF(q, i\nu_m)}, \quad (5)$$

where $F(q, i\nu_m)$ is the Lindhard function. The ladder diagram contribution to the phonon self-energy of Fig. 1(c), $\Pi_{\text{L}}(q, i\nu_m)$, is given by

$$\Pi_{\text{L}}(q, i\nu_m) = -\frac{1}{\beta^2} I^2 \sum_{kk'} \sum_{nn'} G^0_k(i\omega_n) G^0_{k-q}(i\omega_{n-m}) \times G^0_{k'}(i\omega_{n'}) G^0_{k'+q}(i\omega_{n'+m}) \times \frac{F(k'-k+q, i\nu_{n'-n+m})}{1 - IF(k'-k+q, i\nu_{n'-n+m})}, \quad (6)$$

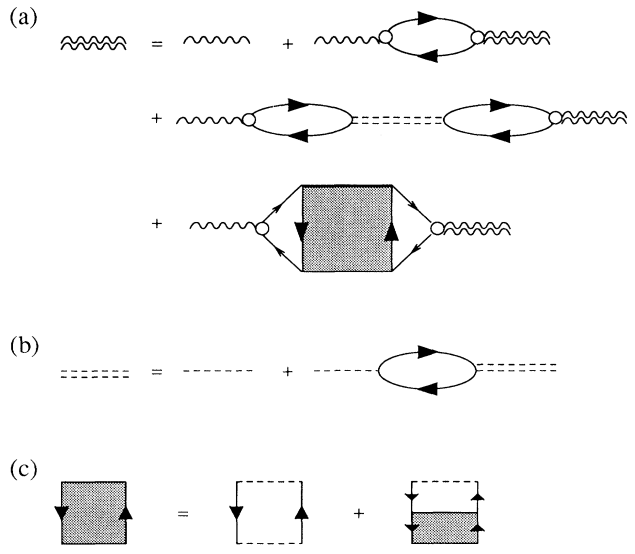

FIG. 1. Diagrams for the phonon Green's function. In addition to the renormalized Coulomb correlation of (b), the contribution from a ladder diagram of (c) is considered in calculating the phonon self-energy.

where $G^0_k(i\omega_n)$ $[= 1/(i\omega_n - \epsilon_k)]$ is the noninteracting electron Green's function. It is too complicated to evaluate $\Pi_{\text{L}}(q, i\nu_m)$ exactly, and so we use here an approximation to get essential features of the diagram. That is, utilizing an idea of the mean value theorem,[4] we take the final term in Eq. (6) out of the summation,

$$\Pi_L(q, i\nu_m) = -\frac{1}{\beta^2} I^2 \alpha(q, i\nu_m) \frac{F(q, i\nu_m)}{1 - IF(q, i\nu_m)} \times \sum_{kk'} \sum_{nn'} G^0_k(i\omega_n) G^0_{k-q}(i\omega_{n-m}) G^0_{k'}(i\omega_{n'}) \times G^0_{k'+q}(i\omega_{n'+m}), \quad (7)$$

with a parameter $\alpha(q, i\nu_m)$. Then, $\Pi_L(q, i\nu_m)$ becomes

$$\Pi_{\text{L}}(q, i\nu_m) = -\alpha(q, i\nu_m) \frac{I^2 F(q, i\nu_m)^3}{1 - IF(q, i\nu_m)}. \quad (8)$$

At the present step, we have no way to get $\alpha(q, i\nu_m)$ exactly. However, $\alpha(q, i\nu_m)$ is expected to be a quantity of $O(1)$, and so we take $\alpha(q, i\nu_m)$ to be unity as a simplest approximation.[9]

As a result, the phonon Green's function $D_q(i\nu_m)$ in Fig. 1(a) satisfies the following Dyson's equation:

$$D_q(i\nu_m) = D^0_q(i\nu_m) + 2|g(q)|^2 D^0_q(i\nu_m) F(q, i\nu_m) D_q(i\nu_m) - 2|g(q)|^2 \frac{I}{1 + IF(q, i\nu_m)} D^0_q(i\nu_m) F(q, i\nu_m)^2 D_q(i\nu_m) - 2|g(q)|^2 \frac{I^2}{1 - IF(q, i\nu_m)} D^0_q(i\nu_m) F(q, i\nu_m)^3 D_q(i\nu_m). \quad (9)$$

From this, we obtain

$$D_q(i\nu_m) = \frac{2\Omega_q}{\nu_m^2 + \omega_q^2}, \tag{10}$$

with

$$\omega_q^2 = \Omega_q^2 - 2\Omega_q |g(q)|^2 \frac{2F(q)}{\epsilon(q)}, \tag{11}$$

where

$$\frac{1}{\epsilon(q)} = \frac{1}{1+IF(q)} - \frac{I^2F(q)^2}{1-IF(q)}. \tag{12}$$

In the derivation, we have taken the adiabatic approximation $F(q, i\nu_m) \simeq F(q,0) \equiv F(q)$ and assumed a paramagnetic ground state [i.e., we consider a situation of $IN(E_F) < 1$] to evaluate $F(q)$. Hence $F(q)$'s above do not have explicit spin dependences.[10]

The renormalized phonon frequency, Eq. (11), for the Hubbard model has a form similar to that for the electron gas model.[4] However, different from the case in the electron gas system, the bare phonon in the present model does not have to be longitudinal ionic plasma. Since the noninteracting electron Hamiltonian in the Hubbard model is considered to be based on the Hartree-Fock approximation,[8] the bare phonon frequency Ω_q in the present model corresponds to the one which is already screened by the Hartree-Fock dielectric function. Thus the bare phonon Ω_q can be assumed to have a proper dispersion relation.[11] Note also that the effect of the Coulomb correlation on the phonon frequency in the Hubbard model is quite different from the exchange effect in the electron gas model. With increasing I, the inverse of the dielectric function, Eq. (12), monotonically decreases, and accordingly ω_q in Eq. (11) becomes larger. Hence the Coulomb correlation interaction in the Hubbard model leads to a phonon hardening rather than a phonon softening, in contrast to the case for the electron gas model. Furthermore, the hardening is reinforced by ladder diagrams taken into account in our case. This finding implies that a charge density wave (CDW) ground state accompanied by a phonon softening may be unlikely in the Hubbard model, especially when the Coulomb correlation interaction is very large.

The static form of the dielectric function in Eq. (12) is easily negative. This property is expected to originate from the intrinsic nature of the Hubbard Hamiltonian. In the Hubbard Hamiltonian, there is only one q-independent parameter, I, describing the electron-electron interaction with opposite spins only. Hence the properties of the dielectric function in the Hubbard model system are very different from those in the the electron gas. The problem of the negative dielectric function in the electron gas system has been studied much in relation to the sum rule.[12] It has been found that negative values of the static dielectric function may appear in the system, in the case of an inhomogeneous electron gas with a strong exchange-correlation interaction. In contrast, the problem of the negative dielectric function and the sum rule for the Hubbard model system has been relatively unexplored. In the Hubbard model system, the form of the dielectric function $\epsilon_{ee}(q)$ which screens the electron-electron interaction is quite different from that of $\epsilon_{ei}(q)$ which screens the electron-ion interaction, even in the level of the random phase approximation. The dielectric function given in Eq. (12) is the one which screens the electron-ion interaction. As a matter of fact, the negative dielectric function of $\epsilon_{ei}(q)$ does not make any problem in the present formalism, since it does not produce any instability, as discussed above for the CDW state.

Using the phonon Green's function, we now evaluate the electron-phonon coupling constant $\lambda_{\rm ph}$. The coupling constant λ can be calculated from the electron self-energy $\Sigma(\omega)$,

$$\lambda = -\partial\Sigma(\omega)/\partial\omega|_{\omega=0}. \tag{13}$$

We consider the diagrams of Fig. 2 for the electron self-energy $\Sigma_{\rm ph}(k,\omega)$, induced by the electron-phonon interaction. Vertices in the diagram represent renormalized electron-phonon interaction matrix elements $\tilde{g}(q)$ due to both electron-phonon and electron-electron Coulomb interactions [see Fig. 2(b)].

We employ in the present study Migdal's theorem to neglect a vertex renormalization by the electron-phonon interaction. Instead, we treat carefully a renormalization by the electron-electron Coulomb interaction. We consider both bubble and ladder diagrams of vertex renormalizations, shown in Fig. 2(b). The inclusion of the ladder diagram in the vertex function is in the same spirit as for the phonon self-energy.[13]

Then $\tilde{g}(q)$ is now given as

$$\tilde{g}(q) = g(q) - g(q)F(q, i\nu_m)\frac{I}{1+IF(q,i\nu_m)} + g(q)\Gamma_{\rm L}(q, i\nu_m). \tag{14}$$

The second term corresponds to a vertex correction due to the bubble diagram, and the third due to the ladder diagram. $\Gamma_{\rm L}(q, i\nu_m)$ represents an approximate vertex correction averaged over incoming and outgoing electron lines:

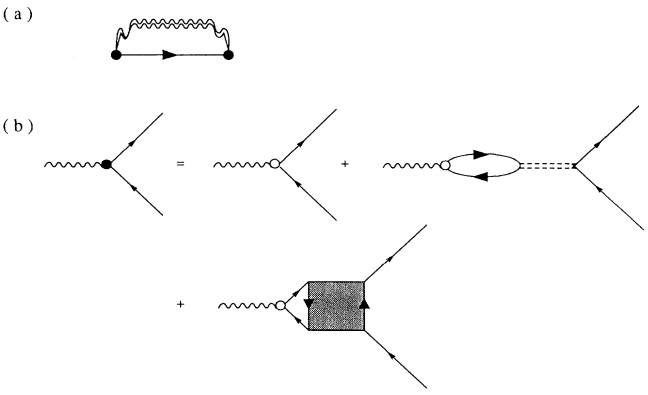

FIG. 2. Diagrams for the electron self-energy due to the electron-phonon interaction. (a) denotes the self-energy diagram and (b) denotes vertex corrections for the electron-phonon interaction matrix element.

$$\Gamma_{\rm L}(q,i\nu_m)=\frac{1}{\beta}I^2\sum_{kk'}\sum_{nn'}G^0_k(i\omega_n)G^0_{k-q}(i\omega_{n-m})G^0_{k'}(i\omega_{n'})G^0_{k'+q}(i\omega_{n'+m})$$
$$\times\frac{F(k'-k+q,i\nu_{n'-n+m})}{1-IF(k'-k+q,i\nu_{n'-n+m})}\frac{1}{\sum_{kn}G^0_k(i\omega_n)G^0_{k-q}(i\omega_{n-m})}. \quad (15)$$

Thus, $\Gamma_{\rm L}(q,i\nu_m)$ no longer depends on the momentum and the frequency of the incoming electron. To calculate $\Gamma_{\rm L}(q,i\nu_m)$, we adopt again the mean value approximation similarly as in the calculation of $\Pi_{\rm L}(q,i\nu_m)$ [Eq. (7)]:

$$\Gamma_L(q,i\nu_m)=-\frac{1}{\beta^2}I^2\bar{\alpha}(q,i\nu_m)\frac{1}{1-IF(q,i\nu_m)}$$
$$\times\sum_{kk'}\sum_{nn'}G^0_k(i\omega_n)G^0_{k-q}(i\omega_{n-m})G^0_{k'}(i\omega_{n'})$$
$$\times G^0_{k'+q}(i\omega_{n'+m}), \quad (16)$$

with a parameter $\bar{\alpha}(q,i\nu_m)$. Then, $\Gamma_{\rm L}(q,i\nu_m)$ becomes

$$\Gamma_{\rm L}(q,i\nu_m)=-\bar{\alpha}(q,i\nu_m)\frac{I^2F(q,i\nu_m)^2}{1-IF(q,i\nu_m)}. \quad (17)$$

Within our approximation scheme, the unknown parameter $\bar{\alpha}(q,i\nu_m)$ can be taken to be unity. By substituting Eq. (17) into Eq. (14), $\tilde{g}(q)$ becomes

$$\tilde{g}(q)=\frac{g(q)}{\epsilon(q)}, \quad (18)$$

with

$$\frac{1}{\epsilon(q)}=\frac{1}{1+IF(q)}-\frac{I^2F(q)^2}{1-IF(q)}. \quad (19)$$

The adiabatic approximation is also used here. Note that the dielectric function for the vertex renormalization, Eq. (19), is exactly the same as that for the renormalized phonon frequency, Eq. (12), reflecting that our procedures of selecting diagrams in Fig. 1 and Fig. 2 are quite consistent. The above result suggests that the absolute magnitude of $\tilde{g}(q)$ becomes strongly enhanced as $IN(E_F)\to 1$, due to the ladder diagram contribution to the vertex correction.

With $D_q(i\nu_m)$ and $\tilde{g}(q)$, $\Sigma_{\rm ph}(k,\omega)$ and $\lambda_{\rm ph}$ can be calculated in a conventional way:[14]

$$\Sigma_{\rm ph}(k,\omega)=\sum_q|\tilde{g}(q)|^2\frac{\Omega_q}{\omega_q}\left[\frac{n(\omega_q)+1-f(\epsilon_{k-q})}{\omega-\epsilon_{k-q}-\omega_q}\right.$$
$$\left.+\frac{n(\omega_q)+f(\epsilon_{k-q})}{\omega-\epsilon_{k-q}+\omega_q}\right] \quad (20)$$

and

$$\lambda_{\rm ph}=N(E_F)\left\langle\left\langle|\tilde{g}(q)|^2\frac{2\Omega_q}{\omega_q^2}\right\rangle\right\rangle, \quad (21)$$

where $n(\omega_q)$ and $f(\epsilon_{k-q})$ are the Bose and Fermi distribution functions, respectively, and $\langle\langle\cdots\rangle\rangle$ denotes an average over the Fermi surface.

For high-T_c superconductors, Migdal's theorem is expected to work because they have rather wide bands obeying Luttinger's theorem. However, the application of Migdal's theorem to narrow band systems, such as heavy fermions, remains to be justified. At present there is no way to calculate the vertex corrections in detail.[15] Pietronero and Strässler[16] have recently claimed that, for narrow band systems which do not satisfy Migdal's theorem, the effect of higher-order electron-phonon vertex corrections produces a strong enhancement of the superconducting transition temperature T_c with respect to T_c from the usual McMillan's theory.[17] They argued that the T_c formula in this case has a different structure from McMillan's formula. Their finding suggests that the estimated T_c based on Migdal's theorem will correspond to a lower limit for a given $\lambda_{\rm ph}$, which is to be increased more when considering the effect of breakdown of Migdal's theorem.

III. COMPARISON OF $\lambda_{\rm ph}$ AND $\lambda_{\rm sf}$

In order to compare $\lambda_{\rm ph}$ with $\lambda_{\rm sf}$, we also evaluate $\lambda_{\rm sf}$ in the Hubbard model. Since a lot of studies have been reported on $\lambda_{\rm sf}$,[3,18] we briefly introduce here a procedure for calculating the self-energy $\Sigma_{\rm sf}(k,\omega)$ and $\lambda_{\rm sf}$. In calculating $\Sigma_{\rm sf}(k,\omega)$, one considers both particle-hole bubble and ladder diagrams.[19] Only an odd number of bubbles should be considered in the bubble diagrams because the bare interaction I connects particles with opposite spins only. The contributions to the electron self-energy from two kinds of diagrams are given as follows:

$$\Sigma^{\rm sf}_{\rm bubble}(k,i\omega_n)=\frac{1}{\beta}\sum_{q,m}G^0_{k-q}(i\omega_{n-m})\frac{I^2F(q,i\nu_m)}{1-I^2F(q,i\nu_m)^2}, \quad (22)$$

$$\Sigma^{\rm sf}_{\rm ladder}(k,i\omega_n)=\frac{1}{\beta}\sum_{q,m}G^0_{k-q}(i\omega_{n-m})\frac{I^2F(q,i\nu_m)}{1-IF(q,i\nu_m)}. \quad (23)$$

With the self-energy $\Sigma^{\rm sf}(k,\omega)$, one can calculate the coupling constant $\lambda_{\rm sf}$. The resulting $\lambda^{\rm bubble}_{\rm sf}$ and $\lambda^{\rm ladder}_{\rm sf}$ are given by

$$\lambda^{\rm bubble}_{\rm sf}=N(E_F)\left\langle\left\langle\frac{I^2F(q)}{1-I^2F(q)^2}\right\rangle\right\rangle, \quad (24)$$

$$\lambda^{\rm ladder}_{\rm sf}=N(E_F)\left\langle\left\langle\frac{I^2F(q)}{1-IF(q)}\right\rangle\right\rangle. \quad (25)$$

The definition of $\langle\langle\cdots\rangle\rangle$ is identical with that in Eq. (21).

The effective (total) spin-fluctuation coupling constant $\lambda_{\rm sf}$ is given by

$$\lambda_{\rm sf} = \lambda_{\rm sf}^{\rm bubble} + \lambda_{\rm sf}^{\rm ladder} - (\text{second-order contribution}), \tag{26}$$

since the second-order contribution is doubly counted in $\lambda_{\rm sf}^{\rm bubble}$ and $\lambda_{\rm sf}^{\rm ladder}$.

We have carried out numerical calculations for Eqs. (21) and (26), assuming a parabolic electron band for ϵ_k. Calculated results are plotted as a function of $IN(E_F)$ in Fig. 3. Figure 3 reveals several interesting features. First, both $\lambda_{\rm ph}$ and $\lambda_{\rm sf}$ increase rapidly as $IN(E_F) \to 1$, reflecting that both coupling constants become enhanced in a strongly correlated system. Second, $\lambda_{\rm sf}$ is larger than $\lambda_{\rm ph}$ for $IN(E_F) > 0.4$, implying that the spin-fluctuation effect dominates over the phonon effect in the correlated regime. It seems thus unlikely that a phonon-mediated BCS superconducting state can be realized in a strongly correlated system.

Our finding of the correlation enhanced $\lambda_{\rm ph}$ in the Hubbard model is consistent with the exchange enhanced $\lambda_{\rm ph}$ in the electron gas model.[4] However, the origins of the enhancement are different from each other. In the electron gas model, both the phonon softening and the screening due to an exchange interaction play roles, whereas in the Hubbard model, the ladder diagram in the vertex function which is not taken into account in the electron gas model gives rise to the enhancement. Remember that the phonon is rather hardened by the correlation in the Hubbard model, which is the reason why $\lambda_{\rm ph}$ in Fig. 3 decreases first with increasing $IN(E_F)$.

MacDonald[20] once pointed out that a shortcoming of conventional ways of evaluating $\lambda_{\rm sf}$ for the Hubbard model is attributed to the use of a parabolic band with an infinite bandwidth. He estimated $\lambda_{\rm sf}$ for Pd which has a finite d band, and found that $\lambda_{\rm sf}$ becomes much smaller than the value obtained with an infinite parabolic band. He took account of a finite bandwidth using a truncated parabolic band for the noninteracting Hamiltonian as follows:

$$H_0' = \sum_{k\sigma} \epsilon_k c_{k\sigma}^\dagger c_{k\sigma} \Theta(k_c - k). \tag{27}$$

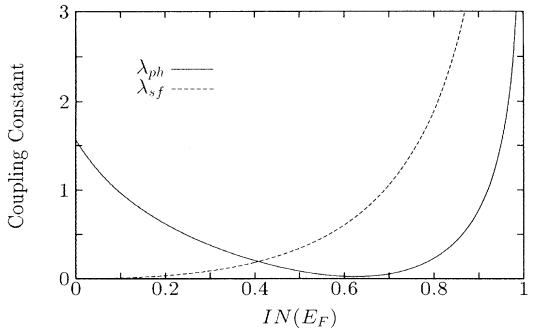

FIG. 3. $\lambda_{\rm ph}$ and $\lambda_{\rm sf}$ as a function of $IN(E_F)$. The original Lindhard function with an infinite parabolic electron band is used. The electron-phonon interaction matrix element is chosen such that $|g(q)|^2 N(E_F)/\Omega_q = 0.22$.

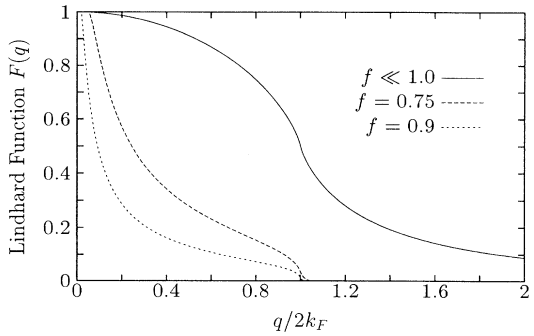

FIG. 4. Comparison of the original Lindhard function and modified Lindhard functions with the finite bandwidth.

A model parameter k_c gives a bandwidth (Θ is the step function), and the fraction of the occupied band corresponds to $(k_F/k_c)^3 \equiv f$. With this modification, the Lindhard function $F(q)$ is accordingly modified in such a way that $F(q)$ becomes much smaller than the original Lindhard function, as $f \to 1.0$ (see Fig. 4).

Note that, in high-T_c superconductors and heavy fermions, spin fluctuations originate from d- and f-band electrons, respectively, which have finite bandwidths. Therefore, it would be essential to take into account the effect of the finite bandwidth in comparing $\lambda_{\rm ph}$ and $\lambda_{\rm sf}$. Employing the modified Lindhard function, we have performed again numerical calculations for $\lambda_{\rm ph}$ and $\lambda_{\rm sf}$ for the case of $f = 0.90$. The results are presented in Fig. 5, which shows that both quantities are reduced a lot in overall magnitudes, as compared to the case of an infinite bandwidth of Fig. 3. Most prominent is the suppression of $\lambda_{\rm sf}$, which becomes smaller than $\lambda_{\rm ph}$ even when $IN(E_F) \to 1.0$. Indeed, when $IN(E_F) = 0.95$, $\lambda_{\rm ph}$ is estimated to be larger than $\lambda_{\rm sf}$ for $f > 0.83$ (see Fig. 6). This finding suggests that, for a correlated material with nearly filled band, $\lambda_{\rm ph}$ becomes larger than $\lambda_{\rm sf}$, so that a phonon-induced superconductivity could be possible in the strong correlated limit [$IN(E_F) \approx 1.0$].

It is anticipated that the present formalism can be applied to high-T_c superconductors, in view of the fact that they have nearly filled bands and are considered to be

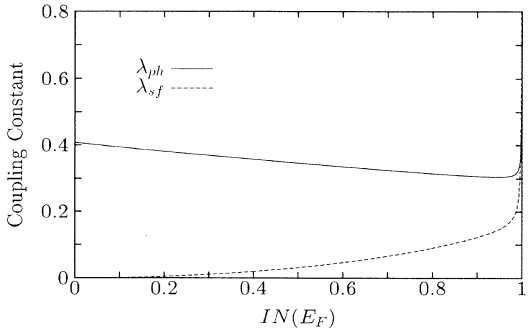

FIG. 5. $\lambda_{\rm ph}$ and $\lambda_{\rm sf}$ as a function of $IN(E_F)$. The modified Lindhard function which takes into account a finite bandwidth with $f = 0.9$ is used.

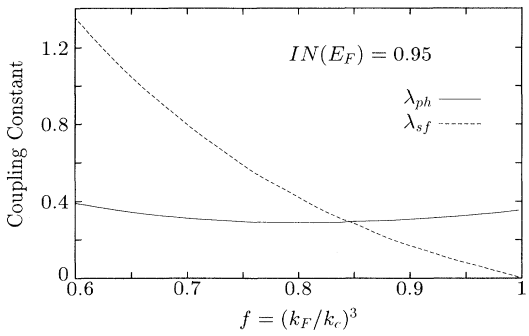

FIG. 6. $\lambda_{\rm ph}$ and $\lambda_{\rm sf}$ as a function of f for $IN(E_F) = 0.95$.

in the vicinity of the magnetic instability. Interestingly, Fig. 6 reveals that $\lambda_{\rm ph}$ is larger than $\lambda_{\rm sf}$ for f corresponding to the occupied band fractions of high-T_c superconductors. A quantitative comparison, however, may not be meaningful, since coupling constants in Fig. 6 were evaluated with a model parabolic band and the assumed $IN(E_F) = 0.95$. More detailed studies incorporating realistic electron and phonon band structures are required. The crucial result of this work is to give evidence that the phonon-induced superconductivity could be possible even in the strongly correlated systems with nearly filled bands, which might have relevance to superconducting mechanisms in high-T_c materials or heavy fermions.

IV. CONCLUSION

In order to investigate the electron-phonon interaction in strongly correlated systems, we have evaluated the phonon self-energy and $\lambda_{\rm ph}$ for the Hubbard Hamiltonian including the electron-phonon interaction. Main results of this paper are as follows. (i) By including the ladder-type diagram for the phonon self-energy, it is found that the phonon becomes hardened with increasing the Coulomb correlation in the Hubbard model, and so a CDW ground state is unlikely in the strongly correlated systems. (ii) Considering the ladder-type diagram for the vertex function of the electron-phonon interaction, we have found that $\lambda_{\rm ph}$ becomes enhanced by the Coulomb correlation in the Hubbard model. (iii) Taking into account an effect of the finite bandwidth, we have found that both $\lambda_{\rm ph}$ and $\lambda_{\rm sf}$ are reduced a lot in overall magnitudes, and that $\lambda_{\rm ph}$ becomes dominant over $\lambda_{\rm sf}$ for a system with a nearly filled band in the strongly correlated limit. Our results indicate that phonon-mediated BCS superconductivity can be possible even in strongly correlated systems such as heavy fermions or high-T_c superconductors.

ACKNOWLEDGMENTS

This work was supported by the POSTECH-BSRI program of the Korean Ministry of Education and also in part by the Korea Science Engineering Foundation through the SRC program of SNU-CTP.

[1] *High Temperature Superconductivity*, Proceedings of Los Alamos Symposium, 1989, edited by K.S. Bedell, D. Coffey, D.E. Meltzer, D. Pines, and J.R. Schrieffer (Addison-Wesley, Redwood City, 1990), and references therein.

[2] See P. Fulde and P. Horsh, Europhys. News **24**, 73 (1993), and references therein.

[3] N. Berk and J.R. Schrieffer, Phys. Rev. Lett. **17**, 433 (1966).

[4] D.J. Kim, Phys. Rev. B **17**, 468 (1978); Phys. Rep. **171**, 129 (1988).

[5] D.J. Kim, Jpn. J. Appl. Phys. **26**, L741 (1987).

[6] J.H. Kim, K. Levin, R. Wentzcovitch, and A. Auerbach, Phys. Rev. B **40**, 11378 (1989); **44**, 5148 (1991).

[7] J.H. Kim and Z. Tesanovic, Phys. Rev. Lett. **71**, 4218 (1993).

[8] J. Hubbard, Proc. R. Soc. London A **276**, 238 (1963).

[9] This approximation is acceptable, considering the fact that the dominant contribution of the ladder diagram comes from low-energy and long-wavelength excitations of the transverse spin fluctuation, that is, excitations with $|\vec{k}' - \vec{k} + \vec{q}| \ll 2k_F$ and $|i\nu_{n'-n+m}| \ll v_F|\vec{k}' - \vec{k} + \vec{q}|$.

[10] Note that our main concern is to investigate the possible phase transition from the normal to superconducting state in the vicinity of the magnetic instability, $IN(E_F) \to 1$. Thus, we assumed a paramagnetic ground state for the normal state of a correlated system.

[11] In the numerical calculation, we have assumed $\Omega_q \propto |g(q)|^2 N(E_F)$, as is often used [see, e.g., D. Fay and J. Appel, Phys. Rev. B **20**, 3705 (1979)].

[12] O.V. Dolgov and E.G. Maksimov, in *The Dielectric Function of Condensed Systems*, edited by L.v. Keldysh, D.A. Kirzhnitz, and A.A. Maradudin (Elsevier, New York, 1989), Chap. 4, and references therein.

[13] A similar kind of diagrams for the vertex function has been introduced by J.A. Herz, K. Levine, and M.T. Beal-Monod [Solid State Commun. **18**, 803 (1976)] to discuss the absence of the Migdal theorem for paramagnons. However, they have not derived a closed form for the vertex function.

[14] G.D. Mahan, *Many-Particle Physics* (Plenum, New York, 1990).

[15] See, for example, P. Fulde, J. Keller, and G. Zwicknagl, in *Solid State Physics*, edited by H. Ehrenreich and D. Turnbull (Academic, New York, 1988), Vol. 41.

[16] L. Pietronero and S. Strässler, Europhys. Lett. **18**, 627 (1992).

[17] W.L. McMillan, Phys. Rev. **167**, 331 (1968).

[18] S. Doniach and S. Engelsberg, Phys. Rev. Lett. **17**, 750 (1966).

[19] B. Menge and E. Müller-Hartmann, Z. Phys. B **82**, 37 (1991).

[20] A.H. MacDonald, Phys. Rev. B **24**, 1130 (1981).